

PAPER • OPEN ACCESS

Understanding the source of acoustic emission signals during the wear of stamping tools

To cite this article: Vignesh V Shanbhag *et al* 2018 *IOP Conf. Ser.: Mater. Sci. Eng.* **418** 012098

View the [article online](#) for updates and enhancements.

Understanding the source of acoustic emission signals during the wear of stamping tools

Vignesh V Shanbhag¹, Bernard F Rolfe², Arunachalam N³, Michael P Pereira²

¹ Institute for Frontier Materials, Deakin University, Geelong, VIC 3220, Australia

² School of Engineering, Deakin University, Geelong, VIC 3220, Australia

³ Manufacturing Engineering Section, IIT Madras, 600036, India

E-mail: vshanbha@deakin.edu.au

Abstract: Stamping tools are prone to wear due to the increased use of advanced high strength steels in the automotive industry. For active monitoring of the wear state of stamping tools using acoustic emission, it is important to establish a correlation between specific wear mechanisms and the acoustic emission signals. An adhesive wear mode (galling), which is commonly observed on the stamping tool, can occur in combination with multiple abrasive wear modes on the workpiece, such as ploughing and cutting. This study will establish a correlation between the sources of the acoustic emission signal to the specific surface wear mechanism observed in the stamping process. Therefore, to investigate the source of acoustic emission signal, sheet metal stamping wear tests were conducted using un-worn and worn tool steel dies (AISI D2) and advanced high strength steel sheet (DP780). Accelerated tribology tests were also conducted using a scratch tester with the same material combination, where galling, cutting and ploughing wear mechanisms were observed. By correlating the acoustic emission features, such as power spectral density from the stamping test and the scratch test, it was observed that the change in the acoustic emission signal observed in the stamping process could be attributed to the galling wear mechanisms. This study contributes to the fundamental understanding of different wear mechanisms in sheet metal forming process, the resulting acoustic emissions, and how these can be utilized to develop active monitoring of the tools in the future.

1. Introduction

Galling, which is an adhesive wear mechanism, is commonly observed in the sheet metal forming process [1]. This wear mechanism can degrade the product quality and affect the mass production. According to ASTM G98-02 [2], galling is a form of localised surface damage occurring at the macroscopic level and arising between the sliding solids which involves plastic deformation and material transfer. In sheet metal forming tools, the galling mechanisms can result in a protrusion of transferred material on the tool surface that can become highly work hardened and cause scratches on the sheet surface [3]. When observing these scratches on the sheet surface, they can be considered as abrasive wear-type mechanisms, such as ploughing or cutting.

Different test methods and analysis procedures have been used to investigate galling on the stamping tools. For example, van der Heide et al. [4] performed experiments using the slider on sheet setup and used the coefficient of friction to represent the severity of galling wear. Podgornik et al. [5] attributed the rapid increase in the coefficient of friction curve to galling initiation in pin on disc experiments. Sindi et al. [6] performed experiments using the slider on sheet setup with an acoustic emission (AE) sensor and attributed the dominant frequency (in the range of 65-126 kHz) to adhesive wear. Hase et al.



[7] used a pin on block setup to investigate the adhesive and abrasive wear using AE and observed the adhesive wear in the frequency range of 1-1.5 MHz and abrasive wear in the frequency range of 0.3-1 MHz.

There have also been several studies examining tool wear directly on an industrial setup using different methods. For example, Bassiuny et al. [8] used a strain sensor for the fault diagnosis of the stamping setup and used energy index as a feature to understand fault conditions. Ubhayaratne et al. [9] used audio sensors for tool wear monitoring in sheet metal stamping and used audio spectra and band power feature to represent the wear level on the tool. Skåre et al. [10] and Shanbhag et al. [11] used an acoustic emission sensor to investigate galling wear in sheet metal stamping. In these studies, burst AE signal was observed during the tool wear and time domain features were used to represent the galling wear. In all of these studies, only one AE sensor was used to study wear on the tool or sheet surface.

Numerous studies have separately focussed on abrasive wear modes using AE. For example, Griffin et al. [12]-[13] correlated the abrasive wear mechanism observed in the grinding process with the AE frequency region. Perfilyev et al. [14] examined the abrasive wear modes on copper and silicon surfaces using AE. However, there is limited or no work that identifies the source of the AE signals observed in the stamping process and how the characteristics of these signals change as the severity of the wear on the stamping tools increase.

To correlate the change in the AE signals with the wear mechanisms, the authors believes it is necessary to have more than one AE sensor due to possibilities of more than one wear mechanism, and the differing mechanisms that can be experienced by the opposing surfaces. Since it is difficult to mount an AE sensor on the sheet surface in the continuous stamping process, additional tribological studies must be performed, which can permit the accommodation of two AE sensors – one on each of the sliding surfaces.

Therefore, to understand the AE signal related to the tool wear of the stamping process, a series of tests were conducted using two special-purpose wear tests. Firstly, accelerated semi-industrial stamping wear experiments were conducted with an un-worn and worn die, using a material combination of D2 steel for the tool and DP780 for the sheet material. Using the same material combination, laboratory-based scratch tests were conducted at low and high scratch depths to obtain no-galling and galling conditions. To understand the source of the AE signal and how these change with increasing wear severity, the AE signal was correlated with observations of the sheet and tool surfaces. Finally, to observe the AE frequency region of the wear, the power spectral density was analysed.

2. Experimental details and methodology

2.1. Stamping and scratch test details.

The stamping experiments were performed on a semi-industrial setup. The setup is explained in detail in the work done by Pereira et al. [15]. The stamping setup employs a progressive die and can closely replicate the continuous stamping processes typically use in the automotive industry. As shown in Figure 1, channel-shaped parts are produced from the tooling and AE sensors are clamped to the removable die inserts to observe the wear conditions of the die inserts. The material for the die insert was AISI D2 steel material, which was rough machined, then through hardened to 55-60 HRC, and subsequently precision ground to achieve a precise fit in the tooling and an accurate die radius profile shape. The blank material used in this study is dual phase steel (grade: DP780) with a thickness of 2 mm. The yield strength and ultimate tensile strength of the blank material in the rolling direction are 450 and 530 MPa, respectively, as measured from quasi-static tensile tests. The parameters for the stamping tests were kept constant for both test scenarios examined (worn and un-worn), and are summarised in Table 1.

A vertical milling machine was customised to perform the scratch tests. The rotation of the spindle of the milling machine was locked during the test. As shown in Figure 2, a Kistler dynamometer was clamped to the bed of the machine and later the blank material (DP780) was clamped to the dynamometer. The end of the tool was conical in shape with a R1.5mm spherical tip and was through

hardened to 55-60 HRC. A distance of 5mm was maintained between the two scratches. The parameters and experimental details for the scratch test are summarised in Table 1.

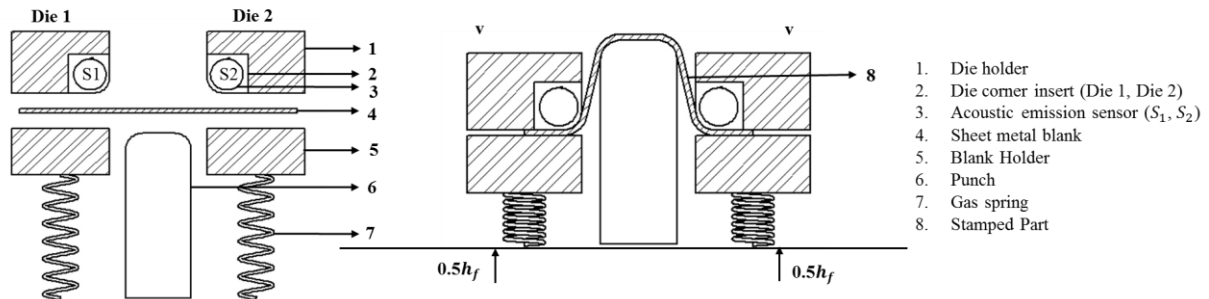


Figure 1. Schematic view of stamping setup a) before stamping b) after stamping.

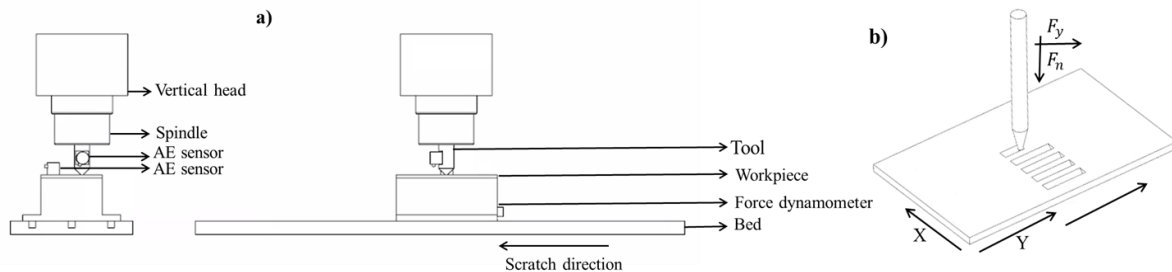


Figure 2. Schematic view of a) scratch test setup b) scratch pin and blank material.

Table 1. Experimental details for stamping and scratch test.

Test type	stamping test	scratch test
Sheet material	DP 780	
Tool material	tool steel (D2)	
Lubricant	dry	
Punch width/tool diameter	30mm	10mm
Tool radius	5mm	1.5mm
Blank thickness	2mm	2mm
Blank width	26mm	100mm
Draw depth/ scratch length	40mm	30mm
Press stroke rate/speed	32 strokes per min	2.7mm/s
Sampling frequency	2 MS/s per channel	
Number of AE sensors	2	

2.2. Profilometry study

The surface examination of the sheet material and tools was performed using an optical profilometer (equipment: Alicona-InfiniteFocus). The objective magnification of 5X and vertical resolution of $1.4\mu\text{m}$ was maintained constant throughout all measurements. As severe wear was observed only on one of the sidewalls of the stamped parts, only one side of the stamped parts, as shown in Figure 3, was examined to understand the wear behaviour of the die radii surface. The sidewalls of the stamped parts were not perfectly flat, therefore the curvature was removed by applying the plane feature available in the profilometer software (IF-MeasurementSuite v5.1) [16]. From the 3D scan obtained from the sidewall surface, the 2D profile is obtained to examine the wear. Similarly, the tool tips used for the scratch test were examined before and after the tests using the optical profilometer to observe the galling on the tool. The scratches obtained were examined for the entire length of 30mm to examine abrasive wear modes.

During the stamping test, the AE sensors were mounted close to the die corner radius (using a magnetic clamp), since the wear is more severe at the radii of the die insert [15]. The AE sensors in the scratch test were clamped on the sheet and tool using a screw clamp. In both the tests, a small amount of ultrasonic couplant (supplier: Cordex; product label: UT 5000) was applied before mounting the AE sensor on the surface. Two wideband AE sensors were used in this study (supplier: Vallen Systeme; model: AE2045S). Each AE data recording was conducted using a sampling rate of 2MHz per channel. The AE sensors were connected to the data acquisition system (supplier: National Instruments; model: PXIe-1078) via a high-speed digitiser (supplier: National Instruments; model: DCPL2) and an AE amplifier (supplier: Vallen Systeme; model: AEP3N) with a gain of 40dB.

A triaxial force sensor load cell (supplier: Kistler; model: Kistler 9257B) was used to acquire the force data during the scratch test. The load cell was connected to the laptop via a multi-channel charge amplifier (supplier: Kistler; Type: 5070A). The sampling rate for the force recording was 5 kHz.

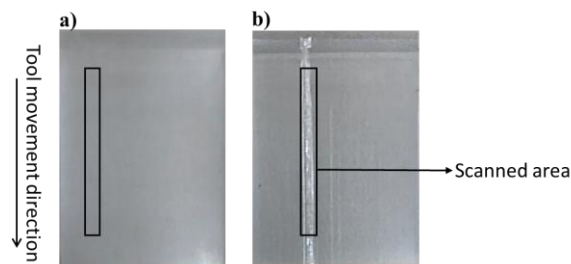


Figure 3. Sidewall of the stamped part using the die a) un-worn b) worn.

2.3. Pencil lead break test

The Hsu-Nielsen pencil lead break test was performed to verify the contact of AE sensor with the surface and to examine the background noise. A 2H lead of 0.5mm diameter was used during the test. For the stamping setup, the test was performed at the die radius. For the scratch setup, the pencil lead break test was performed twice – first on the tool and second on the workpiece – with the tool indented in the sheet. This permitted the observation of the AE signal on both the tool and the workpiece for both pencil lead break tests. From Figure 4 a, we can observe the amplitude of the background noise on the stamping setup is negligible compared to the maximum amplitude observed due to the pencil lead break. From Figure 4 b-c, we can observe the effect of background noise on the test is minimal. However, the AE amplitude was observed to be low from the AE sensor on workpiece compared to the AE amplitude observed from the AE sensor on the tool (Figure 4 b). This indicates that not all events taking place on tool may be captured from the AE sensor on the workpiece. This may be because of the distance between the two AE sensors and the attenuation of the AE signal at the interface of the tool into workpiece [17]-[18]]. A similar trend was observed for the tool during the pencil lead break test on the workpiece. Therefore, two AE sensors are required to understand the wear events taking place on the tool and workpiece.

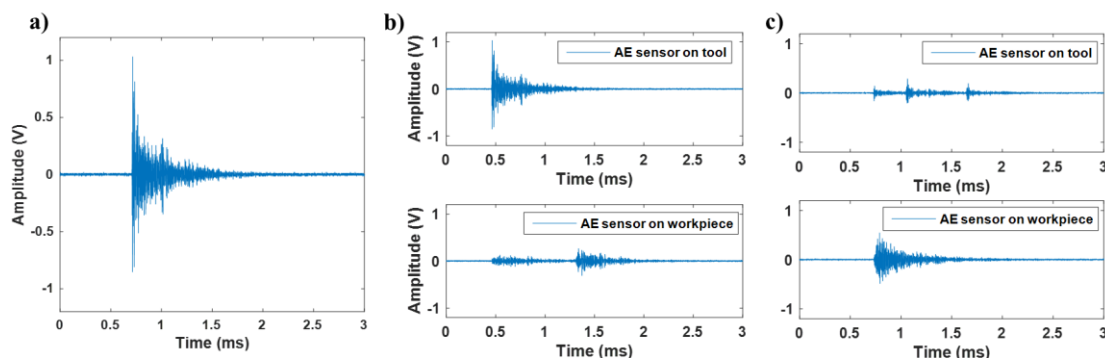


Figure 4. Pencil lead break test on: a) stamping tool, b) scratch test tool and c) scratch test workpiece.

2.4. AE signal for stamping and scratch test

Due to the use of the progressive die in the stamping setup, multiple operations were performed during the single cycle of the stamping process – i.e. each cycle consists of clamping, piercing, stamping and trimming. Based on the timing of the operation, the AE signal related to stamping process could be identified. Detailed explanation of the AE cycle is given in the previous work of Shanbhag et al. [11]. Since this work is focused on the die wear of the stamping process, only the AE signal related to stamping is used for further analysis. Figure 5 represents the AE signal of the stamping process with the un-worn and worn die.

During the scratch test, the AE signal related to the scratch test was identified based on the timing of the force signal. Figure 6 represents the force and AE signals for the scratch test with a vertical displacement (scratch depth) of 0.1 and 0.3mm. This AE signal is used for further AE analysis and to obtain a correlation with the wear events occurring on the tool and sheet surfaces.

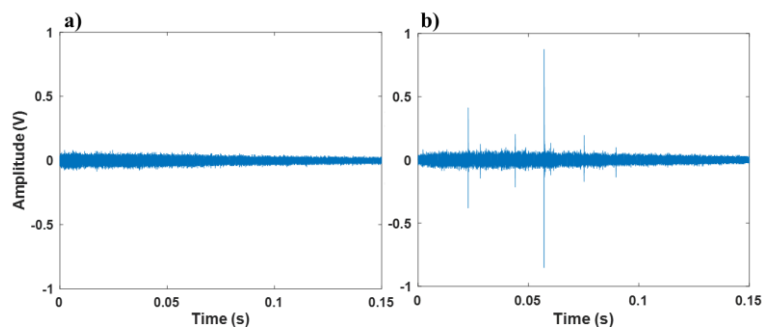


Figure 5. AE signal of the stamping process with die a) un-worn b) worn.

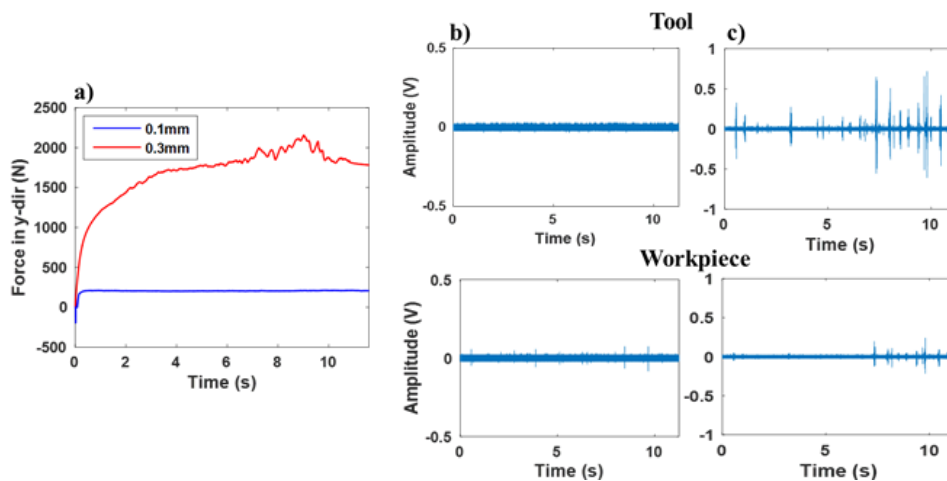


Figure 6. a) Friction force. AE signal for tool and workpiece with depth of b) 0.1mm c) 0.3mm.

2.5. Time and frequency based analysis

The AE analysis performed in this study includes time- and frequency-based studies. These features have been extensively discussed in the literature for other applications [19][20]. A number of time domain and frequency-based feature were examined for the stamping and scratch AE signals, which includes AE RMS, peak, kurtosis, skewness, mean frequency. However, based on the qualitative comparison with the wear profile, only the AE RMS and peak were used further for the analysis and discussion.

Power spectral density has been successfully used for wear studies for other applications [21]-[22]. Therefore, to observe the wear correlation between the stamping and scratch test, the AE signal is further analysed by examining the power spectral density versus frequency plot.

3. Results and discussion

3.1 Profilometry measurements

Figure 7 a, describes the surface profile of the stamped part for the un-worn and worn condition of the die insert. Figure 7 b, describes the surface profile of the scratch groove for the two scratch depths examined – 0.1mm and 0.3mm depths. These correspond to no-galling and galling conditions, respectively. From Figure 7 a, we can observe that the profile for the worn condition shows a large increase in roughness, which may due to galling wear. Similarly, Figure 7 b shows an large increase in roughness for the profile for the larger scratch depth, which correlates with the large amount of galling observed on the indenter.

Figure 8 describes the image of the scratch tool for no-galling (Figure 8 b) and galling conditions (Figure 8 c). By qualitatively correlating, the surface profile measurement for the scratch groove of 0.1mm (blue curve in figure 7 b) with the image of the scratch tool (Figure 8 b), we can observe the small amount of lump has not caused a change in ploughing mode on the sheet surface. This may be due to minimal impact of the initial stages of galling where the lump is not hardened. Whereas, the significant lump observed on the scratch tool for 0.3mm (figure 8 c) may have contributed in the transition of ploughing to cutting abrasive wear on the sheet surface (the red curve in figure 7 b, after 15mm).

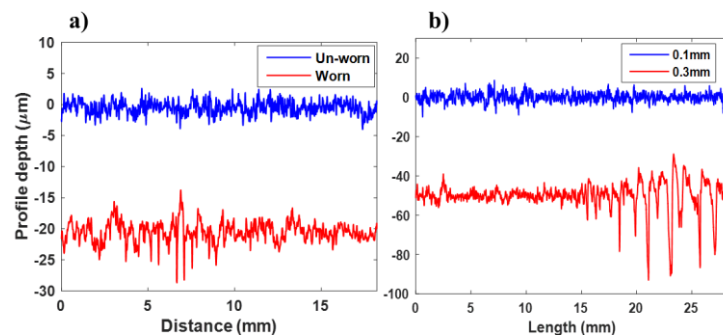


Figure 7. Surface profile along sliding direction of: a) stamped parts and b) scratch grooves.

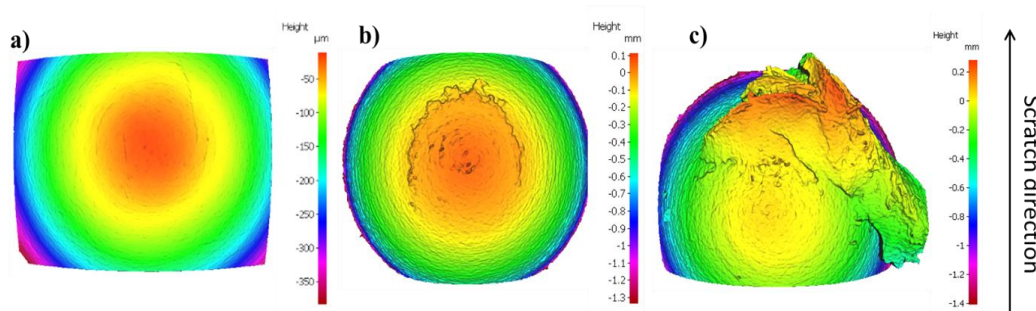


Figure 8. Profilometry measurement: a) un-worn, b) 0.1mm scratch depth, c) 0.3mm scratch depth.

3.2 AE features for stamping process and scratch test.

The AE features for the stamping and scratch test are presented in Table 2. The AE time domain features for worn stamping and galling scratch test conditions (0.3mm) are higher, compared to that of un-worn stamping and no-galling scratch test conditions (0.1mm), respectively. The AE mean-frequency for un-worn stamping and no-galling scratch test conditions is higher compared to that of worn stamping and galling scratch test conditions. Bassiuny et al. [8] attributed this trend to the resonance frequency components exhibited at a lower frequency, which results in a reduction of AE mean frequency for worn and galling scratch test conditions. These features demonstrate the suitability of the AE features for the wear identification. Therefore, AE features such as Peak and RMS were used to study wear progression for the AE signal of the scratch tests.

From Figure 7 b, we can observe the cutting and ploughing condition on the workpiece and in Figure 8 c we can observe a significant adhered lump on the tool. Since cutting, ploughing and galling are observed for this test condition, the AE signal is examined using RMS and peak to correlate with the surface measurements. Figure 9 represents the AE RMS and peak for the scratch test performed at 0.3mm scratch depth. By qualitatively correlating the AE features and the surface profile measurements, we can observe that the large increase in AE features observed after 7 seconds is due to the cutting wear mechanism. However, the few peaks observed in the AE feature before 7 seconds may be attributed to the material pile up at the front of the tool. According to Zhou et al. [23], the AE burst signal is observed due to the release of a large amount of deformation energy stored in the pileup material at the front end of the tool. The AE features for the workpiece is significantly less compared to that of the tool, which possibly indicates the AE features of the tool is mainly due to galling.

Table 2. AE features for the stamping and scratch test.

Test method	Condition & sensor position	RMS (V)	Peak (V)	Kurtosis	Skewness	Mean-frequency (MHz)
Stamping	Un-worn tool	0.0146	0.0809	3.8398	-0.0530	0.2298
	Worn tool	0.0197	0.8744	111.0362	0.0953	0.2021
Scratch	0.1mm depth on tool	0.0060	0.0288	2.9557	-0.0264	0.4789
	0.3mm depth on tool	0.0066	0.7178	136.75	0.1226	0.4293
	0.1mm depth on sheet	0.0061	0.0737	3.0123	-0.0575	0.4579
	0.3mm depth on sheet	0.0061	0.2396	4.1367	-0.0616	0.4616

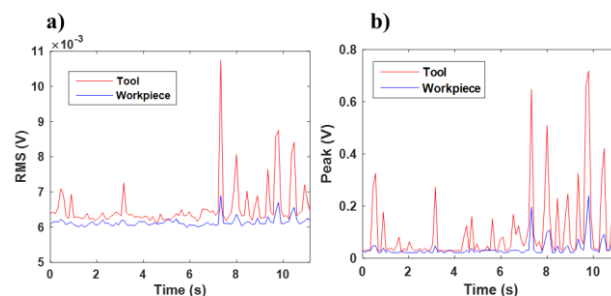


Figure 9. AE features of 0.3mm scratch test: a) RMS, b) Peak.

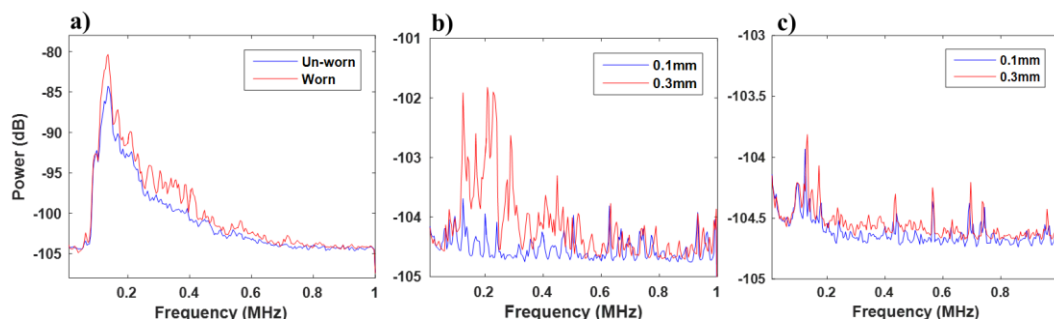


Figure 10. Power spectral plot for a) stamping b) scratch tool c) scratch workpiece

To further examine the effect of galling, the power spectrum is plotted for the AE signal of stamping and scratch test. Figure 10 represents the power spectrum for the AE signal of stamping and scratch test. From Figure 10 a-b, we can observe the wear information for the stamping and scratch tests is

concentrated in the AE frequency region of 0.1-0.5 MHz. In Figure 10 b-c, the AE frequency region for the scratch tests for is 0.1-0.5 MHz for the tool and 0.1-0.2 MHz for the workpiece. This indicates the galling wear on the tool occurs at a higher frequency region, while abrasive wear modes like cutting and ploughing on the sheet occurs at a lower frequency region. These results are in agreement with the study done by Hase et al. [7], where the author observed adhesive wear in the higher frequency range and abrasive wear in the lower frequency range. However, the frequency ranges do not match, which will be the subject of further investigation.

4. Conclusion

This work investigated the source of AE signals observed in the stamping process and aimed to relate these to the severity and mechanisms of wear observed. To meet this aim, a combination of special-purpose scratch tests and stamping tests were conducted.

- During the scratch tests conducted with a scratch depth of 0.1mm, low amplitude AE signals were observed. This was attributed to the fact that, at low scratch depth, the adhesive wear (galling) and abrasive wear (cutting) mechanisms observed were mild, as evident from the surface examination of the tool and workpiece.
- During the scratch tests conducted with a scratch depth of 0.3mm, high amplitude AE signals were observed. These were attributed to the severe adhesive wear (galling) and abrasive wear (cutting) observed at the surface of the tool and workpiece.
- From the power spectral density for the scratch and stamping tests, it was observed that galling results in AE signals in the frequency range of 0.1-0.5MHz. Conversely, abrasive wear on the workpiece results in AE signals in the frequency range of 0.1-0.2 MHz.
- Severe galling wear was observed on the die in the stamping tests and on the indenter in the scratch tests. These corresponded to severe scratches on the opposing sheet surfaces in these tests. Observation of these scratches on the sheets showed abrasive wear modes of ploughing and cutting.

References

- [1] Gåård A, Krakhmalev P V, Bergström J and Hallbäck N, 2007. *Tribo. Lett.* **26**(1), 67-72.
- [2] G98-02, 2008. In ASTM Annual Book of Standards. **03**
- [3] Karlsson P, Gåård A, Krakhmalev P. and Bergström J, 2012. *Wear*, **286**, 92-97.
- [4] Van der Heide E and Schipper, D J, 2003. *Wear*, **254**(11), 1127-1133.
- [5] Podgornik B, Hogmark S and Pezdirnik J, 2004. *Wear*, **257**(7-8), 843-851.
- [6] Sindi C T, Najafabadi M A and Salehi M, 2013. *Tribo. Lett.* **52**(1), 67-79.
- [7] Hase A, Mishina H and Wada M, 2012. *Wear*, **292**, 144-150.
- [8] Bassiuny A M, Li X and Du R, 2007. *Int. J. of Mac. Tools and Manu.*, **47**(15), 2298-2306.
- [9] Ubhayaratne I, Pereira M P, Xiang Y. and Rolfe B F, 2017. *Mech. Systems and Signal Proc.* **85**, 809-826.
- [10] Skåre T and Krantz F, 2003. *Wear*, **255**(7), 1471-1479.
- [11] Shanbhag V, Pereira M, Rolfe B and Arunachalam N, 2017, September. In *Jour. of Phy: ConfSeries.* **896** (1).
- [12] Griffin J and Chen X, 2008. *Int. Jour. of Abrasive Tech.*, **2**(1), 25-42.
- [13] Griffin J and Chen X, 2008. *Int. Jour. of Abrasive Tech.*, **2**(1), 43-59.
- [14] Perfilyev V, Lapsker I, Laikhtman A. and Rapoport L, 2017. *Tribology Letters*, **65**(1), 24.
- [15] Pereira M P, Weiss M, Rolfe B F and Hilditch T B, 2013. *Int. J. of Mac. Tools and Manu.*, **66**, 44-53.
- [16] *IF-MeasurementSuite 5.1*. Retrieved on Jan 21, 2017. <https://www.ita-polska.com>.
- [17] Surgeon M and Wevers M, 1999. *Materials Science and Engineering: A*, **265**(1-2), 254-261.
- [18] Sause M G, 2013. *Journal of Acoustic Emission*, **31**(1), 1-18.
- [19] Lei Y, He Z, Zi Y and Chen X, 2008. *Mechanical Systems and Signal Processing*, **22**(2), 419-435.
- [20] Wang L, Zhang L and Wang X Z, 2015. *Journal of Central South University*, **22**(12), 4625-4633.
- [21] Tandon N and Choudhury A, 1999. *Tribology international*, **32**(8), 469-480.
- [22] Bohse J, 2000. *Composites science and technology*, **60**(8), 1213-1226.
- [23] Zhou W, He Y and Lu X, 2016. *Insight-Non-Destructive Testing and Condition Monitoring*, **58**(5), 256-263.